Chapter 29
FOS Instrument Overview

In This Chapter...

The Faint Object Spectrograph (FOS) was designed by the FOS Investigation Definition Team (IDT) consisting of Richard J. Harms (Principal Investigator), Roger Angel, Frank Barko, Edward Beaver, Ralph Bohlin, Margaret Burbidge, Arthur Davidsen, Holland Ford, and Bruce Margon. The instrument was built by the University of California, San Diego and prime subcontractor Martin Marietta Corporation Aerospace Division. A general overview of the instrument is given in Harms et al., 1982, in *The Space Telescope Observatory,* ed. by D.N.B. Hall (Washington:NASA), p.55.

There have been significant improvements in our understanding of the FOS. *All FOS data should be recalibrated fully* to assure that the latest and most accurate calibration files and the best algorithms are used.

This part of the *HST Data Handbook* describes the basics of the FOS and is the main source of modern information for understanding, recalibrating, and analyzing FOS spectra. References to more detailed information from other sources—appropriate only for the most expert users and unusual situations—are also provided.

We expect that, as more time passes since the removal of the FOS from HST in February 1997, the predominate users of these chapters will be archival researchers. These investigators may not be as familiar with FOS data and its

assessment, calibration, and analysis as the original General Observers (GOs). Accordingly, we have included more detail about instrument operation, data assessment, and calibration than in previous versions of this handbook.

Five chapters are included in the FOS section:

- Chapter 29 gives a summary of the important sources of FOS information, apart from this handbook, a description of the instrument, an overview of the operational history and features of the FOS, and a brief introduction to FOS data-taking modes.
- Chapter 30 describes the basic structure of each important type of FOS data file. We present an overview of how to assess the quality of an FOS observation with detailed reference to the FOS paper products that have been re-designed to facilitate this activity. There are also examples of how to compare a planned observation with the dataset returned from the executed observation for the purpose of understanding anomalies.
- Chapter 31 includes a description of how data are calibrated in the Routine Science Data Processing (RSDP) pipeline and recalibrated with STSDAS, problems that can arise in this procedure, and how you should recalibrate your data with updated calibration files.
- Chapter 32 describes error sources and gives a statement of calibration accuracies.
- Chapter 33 considers several individual data analysis topics including description of some FOS-specific STSDAS tasks.

Although FOS was retired as an active instrument, STScI continues to provide analysis support for FOS data. Questions should be sent to `help@stsci.edu`. Any future updates to FOS documentation and calibration will be announced in the HST Spectrographs Space Telescope Analysis Newsletter (STAN).

29.1 FOS Documentation

In this section we list important sources of documentation for the FOS and its various types of output data.

29.1.1 Instrument Handbooks

Six versions of the *FOS Instrument Handbook* were written. Two of these—the updated pre-launch edition, version 1.1, and the last, version 6.0—exist as electronic documents (currently available only in PostScript format on the FOS WWW Documentation page).

Version 6.0 is the most complete and accurate description of the capabilities of the instrument and practical information for its use. For example detailed discussions of target acquisition procedures, their specificity, and their limitations were included. Version 1.1 gives an excellent and thorough technical-level

description of the instrument. The other versions contain little additional useful information.

29.1.2 Instrument Science Reports

Instrument Science Reports (ISRs) are technical reports that describe calibrations, anomalies, and operational capabilities of the instrument. ISRs are generally written for a technical audience, so we have tried to incorporate the relevant results into this handbook. When an ISR may be particularly helpful, as in treatment of a topic beyond the scope of this volume, we provide the appropriate reference. Most ISRs are available on the FOS WWW Documentation page. Paper copies of all ISRs are available from the STScI Help Desk and can be obtained through `help@stsci.edu`.

29.1.3 WWW Resources

The FOS WWW pages are accessible from the main STScI WWW page and are the primary repository of all FOS information and documentation. A wide variety of documentation, including this handbook, FOS news updates, reference file guides, frequently asked question (FAQ) lists, Calibration Workshop papers, and ISRs can be found here. The FOS WWW page is directly available at:

`http://www.stsci.edu/ftp/instrument_news/FOS/topfos.html`

29.2 General Outline for Handling FOS Data

A brief outline of the steps suggested for an FOS project follows:

1. Select data for retrieval from HST Archive.
2. Examine the data in StarView. (FOS paper products could also be used for an initial quick look).
3. Recalibrate *all* data to benefit from the latest calibration updates and **calfos** enhancements, as described in Chapter 31 (which includes a calibration checklist).
4. Run FOS paper products to evaluate data quality and anomalies. (Refer to the exposure logsheet or RPS2 (RPSS) Phase II specifications if desired).
5. Analyze your data.

You must have some basic knowledge of the FOS and its capabilities in order to refine your archive data search. The remaining sections of this chapter provide an overview of the FOS and, for certain very detailed information, direct you to other sources of information such as the *FOS Instrument Handbook*.

On the basis of your understanding of FOS modes and capabilities you will search the Archive and retrieve observations that may meet your objectives. Using StarView to browse and retrieve data from the Archive is described in Chapter 29.

StarView provides an easy way to quickly assess prospective data, reflecting the original post-observation calibration. Large sets or bulk retrievals can be assessed efficiently at your site with the FOS paper products.

Next, you must recalibrate the observations to obtain the benefit of the FOS closeout calibration and algorithm updates. The accuracies of any FOS data stored in the HST Archive will be improved by recalibration. Chapter 31 describes the recalibration process.

After recalibrating the data, you will want to assess the results and understand the limitations of the calibration as they apply to your data. The FOS paper products, described in Chapter 30, are useful for this purpose. After you evaluate your overall data quality with the paper products you should refer to the description of error sources and accuracy limitations found in Chapter 32. Occasionally, the details of the original observation strategy can be useful in understanding calibration limits for particular types of data. Referring to the exposure logsheet and the data quality assessment material in Chapter 30 may help.

Analyze your data. Although the major focus of this handbook is on understanding FOS calibrations and their accuracies as applied to your data, a few routines that may be useful for specific types of analysis of FOS data are discussed in Chapter 33.

29.3 FOS Instrument Basics

This section provides the basic information needed to understand the geometry and operation of the FOS instrument and the optical components affecting the light path. *FOS Instrument Handbook* versions 1.1 and 6.0 give more details about the instrument performance and capabilities. The final sections of this chapter are summary discussions of each FOS target acquisition and science observing mode.

29.3.1 FOS History and the Introduction of COSTAR

The FOS operated successfully throughout its six-year mission on HST. There were however a number of major milestones during that period, most notably the installation of COSTAR, which corrected the effects of primary mirror aberration for the FOS. Table 29.1 summarizes the most important HST milestones that affected FOS.

During the summer of 1991 (part of the Science Verification (SV) period) substantial changes in certain FOS photocathode granularity patterns (flatfields) were observed, particularly for FOS/RD. Detailed monitoring during the remainder of the period prior to the First Servicing Mission (January 1, 1992,

through December 15, 1993) revealed moderate variations in flatfield combined with overall time- and OTA focus-dependent changes in instrument sensitivity.

The aberration of the primary mirror affected FOS acquisitions and science observations. Modifications to ACQ/BINARY procedures to compensate for the extended PSF wings reduced the likelihood of target acquisition failure by early 1992, but throughout the pre-servicing period aberration-related *crowded field* acquisition failures occurred. The FOS geomagnetically-induced image motion (GIM) was discovered early in SV. In addition to photometric effects, this motion degraded the accuracy of ACQ/BINARY target acquisitions until the implementation of an onboard compensation algorithm in April, 1993.

Y-bases were monitored and regularly updated throughout the FOS operational lifetime. Temporal trending of some FOS y-bases was established by the summer of 1993 and subsequent updates included predicted values based upon the observed trending.

Installation of the Corrective Optics Space Telescope Axial Replacement (COSTAR) on the spacecraft in December of 1993 corrected the effects of spherical aberration of the HST primary mirror on the FOS. COSTAR deployed two correcting mirrors, M1 and M2, into the optical path of FOS. The COSTAR mirrors introduced a modest anamorphic magnification which differed by approximately two percent between the COSTAR *x* and *y*. Aperture and pixel sizes decreased to approximately 0.86 of their pre-COSTAR values. COSTAR restored the design PSF at a modest cost in efficiency attributable to the two corrector reflections. Additional information concerning the impact of COSTAR on FOS is in “Influence of COSTAR on FOS Data” on page 29-19.

Other updates were made to either improve or extend various aspects of instrumental operation and calibration. These included commanding updates to improve the efficiency of ACQ/PEAK, to enhance the brightness dynamic range and reduce the failure rate of ACQ/BINARY, and to enable the use of ACQ/PEAK for moving target acquisitions. Software updates to implement scattered light correction, correctly calibrate OBJ-OBJ observations, and substantially improve flux calibration were also implemented.

29.3.2 Optical Layout

Figure 29.1 shows an optical layout of the FOS. Light entered the FOS through a pair of entrance ports roughly 490" off the optical axis of HST. The light from the object of interest then passed through one of the two independent optical channels, each of which focused nearly stigmatic spectral images on the photocathode of a photon-counting Digicon detector. These two channels differed only in the wavelength sensitivity of their respective detectors, and were referred to as FOS/RD (or Red Side) and FOS/BL (Blue Side). The FOS aperture wheel, located at the HST focal surface, contained separate sets of single or paired apertures (including one blank for background measurements) for each detector which ranged in size from 0.1" to 4.3" (pre-COSTAR) projected onto the sky. From the aperture wheel the optical beam then passed through the polarization analyzer (which included a clear aperture for non-polarimetric observations) and

Table 29.1: Important Dates in FOS History

Date	Event
April 1990	HST launched with FOS onboard
January 1, 1992	SV ends (updated reference files, aperture locations and sizes, and y-bases)
After July 1, 1992	FOS calibration observations commence use of high-precision ACQ/PEAK (0.025" accuracy each coord)
April 5, 1993	Onboard GIM correction implemented
June 1993	ACQ/BINARY 8-steps to success implemented (11 groups became success, not failure)
December 1993	Servicing Mission (SM) 1
About January 1, 1994	COSTAR FOS M1, M2 mirrors deployed
January 1-26, 1994	Calibration of COSTAR-assisted FOS; no FOS observations in this period are formally calibrated due to many different COSTAR mirror positions
February 1, 1994	FOS COSTAR mirrors properly positioned - photometry now possible
March 21, 1994	Scattered light correction algorithm implemented in pipeline
May 30, 1994	FOS post-COSTAR aperture locations updated; SMOV ends
July 1994	More efficient ACQ/PEAK including moving targets implemented
July-November 1994	No header ACQ/PEAK scan parameter information (FOS paper products will not work for ACQ/PEAK taken in this time period)
November 1994	GHRS/FOS acquisition assists initiated
December 1994	Reuse_target_offset implemented
February 5, 1995	Jitter files routinely provided on GO tapes and placed in archive
January 15, 1996	Improved scattered light correction algorithm implemented
March 17, 1996	AIS flux calibration implemented in pipeline
February 13, 1997	FOS removed from HST

on to the grazing incidence mirror, a *roof* prism, which deflected the beam 22 degrees upward. This deflection was required in order to allow the apertures to be placed near the HST optical axis to minimize astigmatism, while meeting the packaging constraints within the FOS. The deflected beam then passed through an order-sorting filter, when required, in the fore part of the filter-grating wheel, and on to an off-axis paraboloidal mirror which collimated the beam and directed it back to the filter-grating wheel. The beam was then dispersed or imaged (for the one imaging position). and focused onto the detector by the selected element on the filter-grating wheel.

29.3.3 Detectors

As described above, the FOS had two Digicon detectors with independent optical paths (Figure 29.1). The Digicons operated by accelerating photoelectrons emitted from a two-dimensional transmissive photocathode onto a linear array of 512 silicon diodes. All 512 FOS diodes were exposed by dispersed light, i.e., none of the diodes were dedicated to background measurement or other purposes. The photoelectron pulses were counted (if a pulse had an amplitude above a programmable threshold) in each of the individual diode channels. A separate microprocessor for each detector controlled the electronics, mechanisms, and Digicons. The counts were summed in microprocessor memory for a mode-dependent preset time and then read from the FOS to the HST computer.

The bi-alkali (Na_2 KSb) blue detector (FOS/BL) photocathode on a magnesium fluoride faceplate was sensitive from 1150 Å to 5400 Å, while the tri-alkali (Na_2 KSb Cs) red Digicon (FOS/RD) photocathode on a fused silica faceplate covered the wavelength range from 1620 Å to 8500 Å. Figure 29.2 shows the quantum efficiencies of both detectors. Note that the graphs in Figure 29.2 are illustrative only; the plotted values are not accurate enough for quantitative use in data analysis. The general characteristics of FOS/BL and FOS/RD are compiled in Table 29.2.

Both photocathodes had spatial irregularities in response (granularity) and localized blemishes that could limit the S/N achieved. These spatially variable features could be removed with appropriate flatfielding provided adequate care was taken in target centering. The diodes themselves also had small response irregularities that were of little consequence and were also removed by routine flatfielding.

Figure 29.1: FOS Optical Path

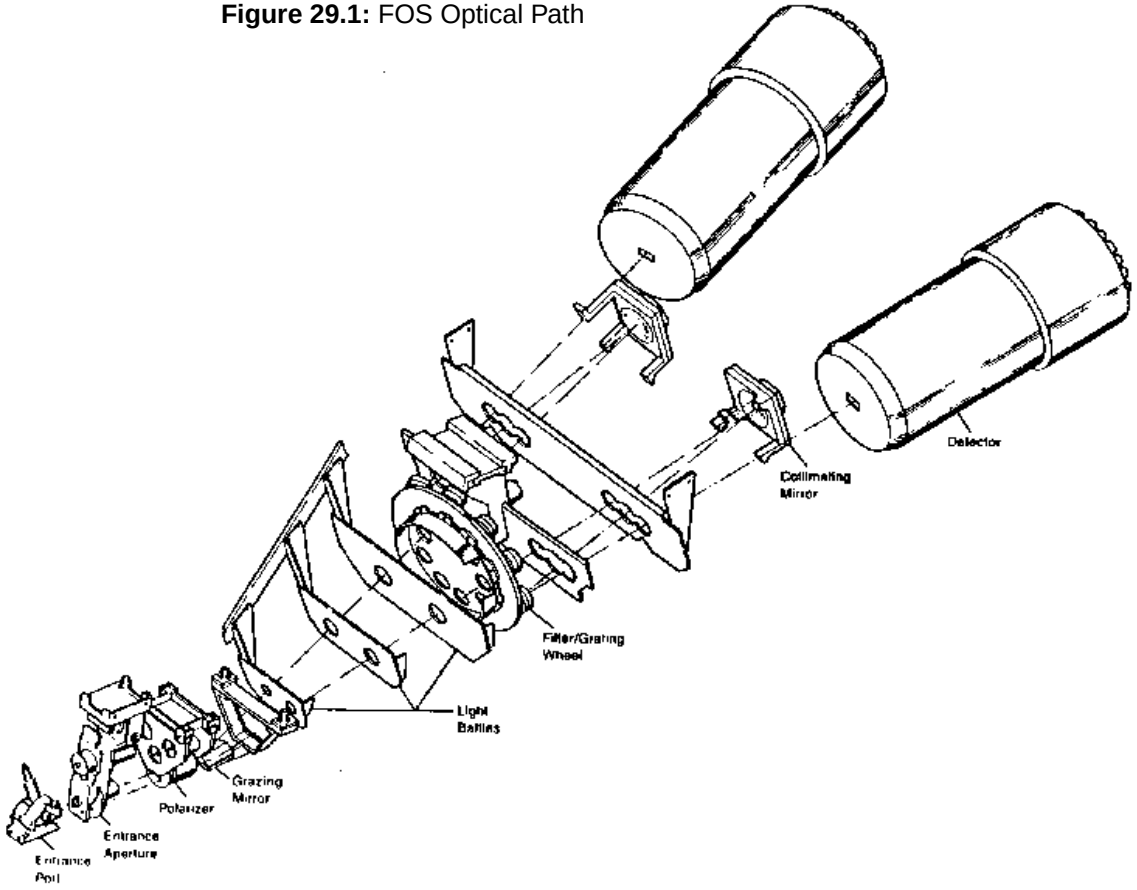

Figure 29.2: Detector Quantum Efficiencies

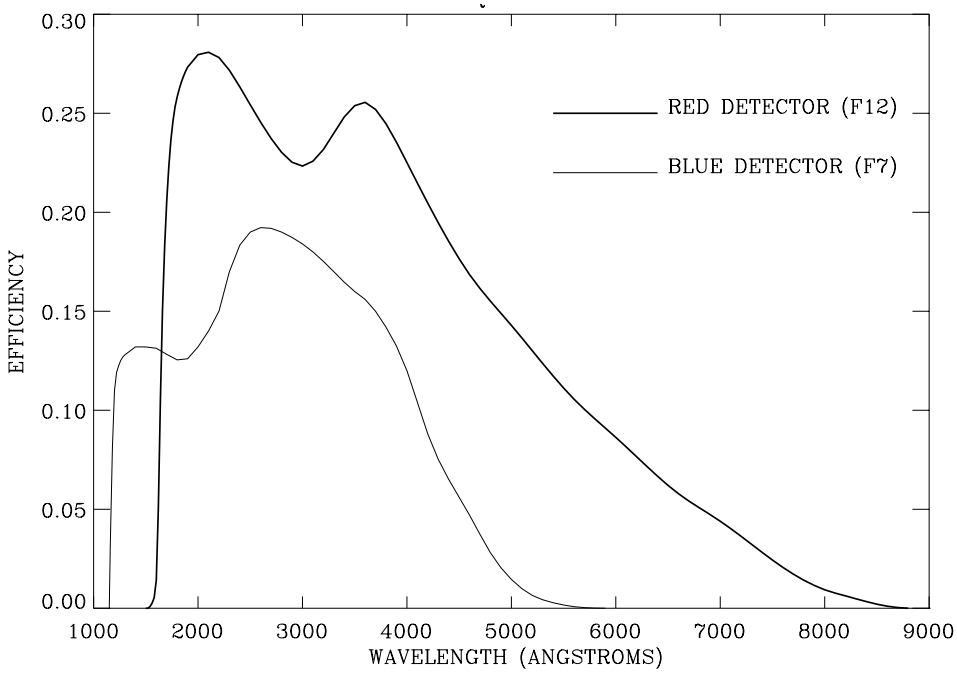

Table 29.2: Detector Characteristics

Attribute	Value
Wavelength coverage	FOS/BL: 1150Å to 5400Å in several grating settings. FOS/RD: 1620Å to 8500Å in several grating settings.
Spectral resolution	High: $\lambda/\Delta\lambda \approx 1300$. Low: $\lambda/\Delta\lambda \approx 250$.
Time resolution	$\Delta t \geq 0.033$ seconds.
Acquisition aperture	4.3″ x 4.3″ (4.3): pre-COSTAR 3.71″ x 3.66″ (4.3) : post-COSTAR
Science apertures	Largest: 4.3″ x 1.43″ (pre); 3.71″ x 1.29″ (post) (4.3). Smallest: 0.09″ square paired (0.1-PAIR).
Diode size	pre-COSTAR: width=0.356″; height=1.43″ post-COSTAR: width=0.305+/-.004″; height=1.291+/-.007″
Plate-scale	pre-COSTAR: FOS/BL and FOS/RD x=y=0.0896″ pixel^{-1} post-COSTAR[a]: FOS/BL x=.0774+/-.001″ pixel^{-1}; y=.0786+/-.001″ pixel^{-1} FOS/RD x=.0752+/-.001″ pixel^{-1}; y=.0812+/-.002″ pixel^{-1}
Mean dark count rate	FOS/BL: 0.0064 counts s^{-1} diode^{-1} FOS/RD: 0.0109 counts s^{-1} diode^{-1}
Example post-COSTAR exposure times 0.9″ (1.0) aperture	F_{1300}=2.5 x 10^{-13}, SNR=20/(1.0Å), t=260s. F_{2800}=1.3 x 10^{-13}, SNR=20/(2.0Å), t=10s (FOS/BL). F_{2800}=1.3 x 10^{-13}, SNR=20/(2.0Å), t=6.6s (FOS/RD).

a. Post-COSTAR telescope movement commanding assumed mean of *x* and *y* values as the mean plate-scale for each detector.

29.3.4 Apertures

The entrance aperture mechanism allowed selection of any one of twelve apertures for each detector. Table 29.3 lists the apertures.

The FOS aperture naming convention was to use the pre-COSTAR aperture size as aperture designation for all observing epochs despite the 16% scale magnification introduced by the COSTAR optics. There was a large aperture for acquiring targets using on-board software (pre-COSTAR: 4.3" x 4.3"; post-COSTAR: 3.7" x 3.7"; designation 4.3[1]). Since the diode array extended only 1.29" (1.43" pre-COSTAR) in the direction perpendicular to the dispersion, this largest aperture had an effective collecting area of 3.7" x 1.29" (pre-COSTAR: 4.3" x 1.43"). Other apertures included several circular apertures with sizes 0.86" (1.0), 0.43" (0.5), and 0.26" (0.3), as well as paired (UPPER and LOWER) square apertures with sizes 0.86" (1.0-PAIR), 0.43"

1. Henceforth, if pre- or post-COSTAR time periods are not specifically stated, we will routinely use post-COSTAR aperture sizes with the pre-COSTAR size aperture designation in parentheses.

Table 29.3: FOS Apertures

Designation (Header Desig.)	Number	Shape	Pre-COSTAR Size (″)	Post-COSTAR Size (″)
0.3 (B-2)	Single	Round	0.30 dia	0.26 dia
0.5 (B-1)	Single	Round	0.50 dia	0.43 dia
1.0 (B-3)	Single	Round	1.00 dia	0.86 dia
0.1-PAIR[a] A-4)	Pair	Square	0.10[a]	0.09[b]
0.25-PAIR[a] (A-3)	Pair	Square	0.25	0.21
0.5-PAIR[a] (A-2)	Pair	Square	0.50	0.43
1.0-PAIR[a] (C-1)	Pair	Square	1.00	0.86
0.25X2.0 (C-2)	Single	Rectangular	0.25 x 2.00	0.21 x 1.71
0.7X2.0-BAR (C-4)	Single	Rectangular	0.70 x 2.00	0.60 x 1.71
2.0-BAR (C-3)	Single	Square	2.00	1.71
BLANK (B-4)	NA	NA	NA	NA
4.3 (A-1)	Single	Square	4.3 x 4.3	3.66 x 3.71[c]
FAILSAFE	Pair	Square	0.50 and 4.3	0.43 and 3.7

a. Pre-COSTAR separation of PAIR apertures was 2.82", whereas post-COSTAR separation was 2.57"; pre-COSTAR aperture positions were assumed symmetric about center of SINGLE apertures. post-COSTAR PAIR “A” apertures were assumed symmetric about center of A-1 and PAIR “C” apertures symmetric about center of C-2.
b. Three of the four A-4 apertures have been consistently measured as one size and the fourth, the FOS/BL LOWER aperture, approximately 25% smaller in each dimension. Due to measurement uncertainties, the FOS/BL LOWER aperture size was determined as ranging from 0.1" (pre-COSTAR) to a size 25% smaller (see *FOS ISRs* 019 and 138).
c. Post-COSTAR size was not the same in both coordinates due to the COSTAR anamorphism (magnification factor in *x* different from that in *y*).

(0.5-PAIR), 0.21" (0.25-PAIR), and 0.09" (0.1-PAIR), for isolating spatially resolved features and for measuring the sky. In addition, a slit and two barred apertures were available (Figure 29.3 and Table 29.3). *Separate aperture sets* existed for FOS/BL and FOS/RD. Aperture size measurements were performed both pre-launch and on-orbit. Precise aperture sizes were reported in

FOS ISRs 019 and 138, for the pre- and post-COSTAR cases, respectively. Aperture positioning repeatability was extremely accurate.

Aperture Center Locations

Before COSTAR was installed, all SINGLE FOS apertures were assumed to be concentric and all spacecraft-centering operations used this assumption. Post-COSTAR SMOV calibrations indicated that the `1.0` and smaller SINGLE apertures were concentric, but that the `4.3` aperture was slightly offset, particularly for FOS/RD, from this center. This offset affected the positional accuracy determined by ACQ/BINARY and required that different flatfields be employed for the `4.3` than for the other SINGLE apertures. The degree of uncertainty in this small offset also affected precise positional determination based upon `4.3` aperture imaging or ACQ/BINARY alone. Pre-COSTAR telescope commanding assumed that the mid-point between each set of paired apertures was concentric with the SINGLE apertures. Post-COSTAR measurements led to the adoption of aperture locations that placed all of the "A" apertures at a common center, all of the "B" apertures (all SINGLE) at a slightly displaced common center, and the "C" apertures at another common center. The `1.0-PAIR` apertures were slightly displaced from all of the other paired apertures and required separate flatfields. The individual components of paired apertures were separated by approximately 2.57". All post-COSTAR telescope commanding after May 30, 1994 included these aperture location offsets.

29.3.5 Dispersers

FOS dispersers provided both "high" spectral resolution (1-6 Å-diode^{-1}, $\lambda/\Delta\lambda \approx$ 1300) and "low" spectral resolution (6-25 Å-diode^{-1}, $\lambda/\Delta\lambda \approx 250$). Their designations and basic properties are presented in Table 29.4. Full optical specification of the FOS dispersers is found in Harms et al., SPIE, 183, 74, 1989 and *FOS ISR* 127. The actual spectral resolution depended on the point spread function of HST, the dispersion, the aperture, and whether the target was physically extended. Representative line widths are given in Table 29.5.

Unlike the apertures, the same dispersers were used with both FOS/BL and FOS/RD. The dispersers and appropriate blocking filters were mounted on the Filter Grating Wheel (FGW) which always rotated in the same direction to specified locations in the beam. Due to the physical nature of the mechanism involved, the repeatability of FGW positioning in the beam was not as precise as for aperture positioning. For certain types of FOS observations, FGW positional uncertainty is an important "error source" (see Chapter 33 and *FOS ISRs* 131, 142, and 145.

29.3.6 Detector Geometry

From the photocathode, electrons were deflected magnetically *without magnification* onto the diode array of the Digicon. In this way the electronic image of the light transmitted by the aperture was projected onto the diode array. The relative size of the different apertures as they were projected onto a section of

the diode array is shown in panel (a) of Figure 29.3, which is displayed from the perspective of an observer positioned directly "behind" the detector looking out toward the sky. The individual diodes were 50 x 200 microns in physical dimension which corresponded to spacings of 0".31 (post-COSTAR) or 0".35 (pre-COSTAR) along the dispersion direction and height of 1".29 (1".43) perpendicular to it. In the FOS detector coordinate system (and throughout this handbook) dispersion lies along the *x-direction*. The *x*-coordinate is always defined positive to the left in the sense of Figure 29.3. Wavelength *always* increased with increasing x for FOS/BL gratings, but always decreased with increasing *x* for FOS/RD gratings and vice versa for the prisms. The *y*-axis of the FOS coordinate frame was perpendicular to the dispersion and was defined positive toward the "top" of the detector as shown. (As one "looks through the detector toward the sky," if east were aligned toward the +*x*-axis, then north was aligned with the +*y*-axis.) The lower paired apertures were closest to the optical axis of HST.

Panel (b) of Figure 29.3 shows three other apertures—two occulting bars and one slit—which were nearly concentric with the 4.3 aperture. Panel (c) shows the orientation of the +*y*-axis in the (V2,V3) plane for the post-COSTAR era.

COSTAR introduced a 180 degree rotation of the telescope (V2,V3) coordinate frame, not the instrument (*x*,*y*) frame. Therefore, before COSTAR, the (V2,V3) coordinate frame was rotated 180 degrees with respect to the orientations shown in Figure 29.3. The angle between FOS/BL and FOS/RD slit orientations (+*y*-directions) was always 73.6 degrees.

The deflection of the photoelectrons was controlled by an internal magnetic field, which in turn depended on a high-voltage setting. The unit of distance in the *y*-direction was the so-called *Y-base unit*. The high voltage was adjusted so that a deflection of 256 Y-base units corresponded to the 200 micron physical height of the diodes (both pre and post-COSTAR). The photocathode coordinate system extended from –2048 to +2048 Y-base units. Each disperser directed incoming light onto a different location on the photocathode as shown in Figure 29.4.

29.3.7 Waveplates and Polarizers

The FOS polarization analyzer positioned one of three elements into the optical path; a clear aperture, a thin magnesium fluroide waveplate (plate "B") plus Wollaston prism assembly, or a thick MgFl waveplate (plate "A") plus Wollaston prism assembly. One waveplate was permanently located in front of each Wollaston, however the waveplate could be rotated so as to alter the position angle of the waveplate fast axis relative to the Wollaston, in increments of 22.5 degrees. The polarimetry appendix of *FOS Instrument Handbook* version 1.1 presents a technical description of the FOS polarimeter.

The technique used for spectropolarimetry in the FOS was very similar to that developed for ground-based instruments. When introduced into the beam, the Wollaston prism assembly produced twin dispersed images of the aperture with opposite senses of polarization at the detector. In order to determine the linear and circular polarization properties of the incoming beam, usually 8 or 16

observations were taken with the waveplate turned in 45 or 22.5 degree intervals relative to the Wollaston prism. This allowed the polarization effects in the dispersing optics following the analyzing prism to be fully removed from the science observations. Waveplate "A" was recommended for use with the disperser G400H and "B" waveplate was recommended for use with the G130H, G190H, and G270H dispersers. Polarizer position "C" (clear) was the default for all non-spectropolarimetric observations.

Table 29.4: FOS Dispersers

Grating	Diode No. at Low λ	Low λ (Å)	Diode No. at High λ	High λ (Å)	Δλ (Å-Diode^{-1})	Blocking Filter
			Blue Digicon			
G130H (H13)	53	1140[a]	516[b]	1606	1.00	–
G190H (H19)	1	1573	516	2330[c]	1.47	–
G270H (H27)	1	2221	516	3301	2.09	SiO_2
G400H (H40)	1	3240	516	4822	3.07	WG 305
G570H (H57)	1	4574	516	6872[d]	4.45	WG 375
G160L (L15)	319	1140[a]	516	2508[c]	6.87	–
G650L (L65)	295	3540	373	9022[d]	25.11	WG 375
PRISM[e] (PRI)	333	1500[f]	29	6000[d]	–	–
			Red Digicon[i]			
G190H (H19)	503	1590[g]	1	2312	-1.45	–
G270H (H27)	516	2222	1	3277	-2.05	SiO_2
G400H (H40)	516	3235	1	4781	-3.00	WG 305
G570H (H57)	516	4569	1	6818	-4.37	WG 375
G780H (H78)	516	6270	126	8500[h]	-5.72	OG 530
G160L (L15)	124	1571[g]	1	2424	-6.64	–
G650L (L65)	211	3540	67	7075	-25.44	WG 375
PRISM[e] (PRI)	237	1850	497	8950[h]	–	–

a. The blue Digicon MgF_2 faceplate absorbed light shortward of 1140 Å.
b. The photocathode electron image typically was deflected across 5 diodes, effectively adding 4 diodes to the length of the diode array.
c. The second order overlapped the first order longward of 2300 Å, but its contribution was at a few percent.
d. Quantum efficiency of the blue tube was very low longward of 5500 Å.
e. PRISM wavelength direction was reversed with respect to gratings of the same detector.
f. The sapphire prism absorbed some light shortward of 1650 Å.
g. The red Digicon fused silica faceplate strongly absorbed light shortward of 1650Å.
h. Quantum efficiency of the red detector was very low longward of 8500 Å.
i. Dispersion direction was reversed for `FOS/RD` relative to `FOS/BL`.

Table 29.5: FOS Line Widths (FWHM) as a Function of Aperture Size

Designation	Size (″)	Aperture Filled with Uniform Source		Pre-COSTAR Point Source at 3400Å FWHM	Post-COSTAR Point Source at 3400Å FWHM
		G130H (Blue) FWHM[a]	G570H (Red) FWHM		
0.3	0.26(circular)	1.00 ± .01	0.95 ± .02	1.06	0.92
0.5	0.43(circular)	1.27 ± .04	1.20 ± .01	1.14	0.93
1.0	0.86(circular)	2.29 ± .02	2.23 ± .01	1.34	0.96
0.1-PAIR	0.09(square)	0.97 ± .03	0.92 ± .02	1.00	0.91
0.25-PAIR	0.21(square)	0.98 ± .01	0.96 ± .01	1.00	0.92
0.5-PAIR	0.43(square)	1.30 ± .04	1.34 ± .02	1.18	0.94
1.0-PAIR	0.86(square)	2.65 ± .02	2.71 ± .02	1.40	0.96
0.25X2.0	0.21 X 1.71(slit)	0.99 ± .01	0.96 ± .01	1.00	0.92
0.7X2.0-BAR	0.60 X 1.71	1.83 ± .02	1.90 ± .01	1.30	1.26
2.0-BAR	1.71	5.28 ± .07	5.43 ± .04	1.40	1.34
4.3	3.66 X 3.71	12.2 ± 0.1	12.2 ± 0.1	1.50	0.96

a. The FWHM are given in units of diodes. A pre-COSTAR diode was 0.356″ wide and 1.43″ high. A post-COSTAR diode was 0.305″ wide and 1.29″ high.

29.3.8 Internal Wavelength Calibration

Two Pt-Ne hollow-cathode lamps provided emission line spectra for calibrating the FOS wavelength scales. The lamp beams passed through the same optics as an external source, but they did not fill the collimator. As a result, it was possible to have an offset in the photocathode position of any particular wavelength in the dispersed internal beam and the dispersed external beam. This internal to external wavelength offset is discussed in more detail in “Wavelength Calibration” on page 32-49. Due to the effect of the FGW positional uncertainty mentioned in “Dispersers” on page 29-11, highly accurate FOS external wavelengths could be determined only with the aid of an internal WAVECAL exposure taken immediately before or after the science exposure with no intervening movement of the FGW.

Figure 29.3: Post-COSTAR Aperture Sizes Projected On Diode Array Viewed from Behind Detector Looking toward Sky

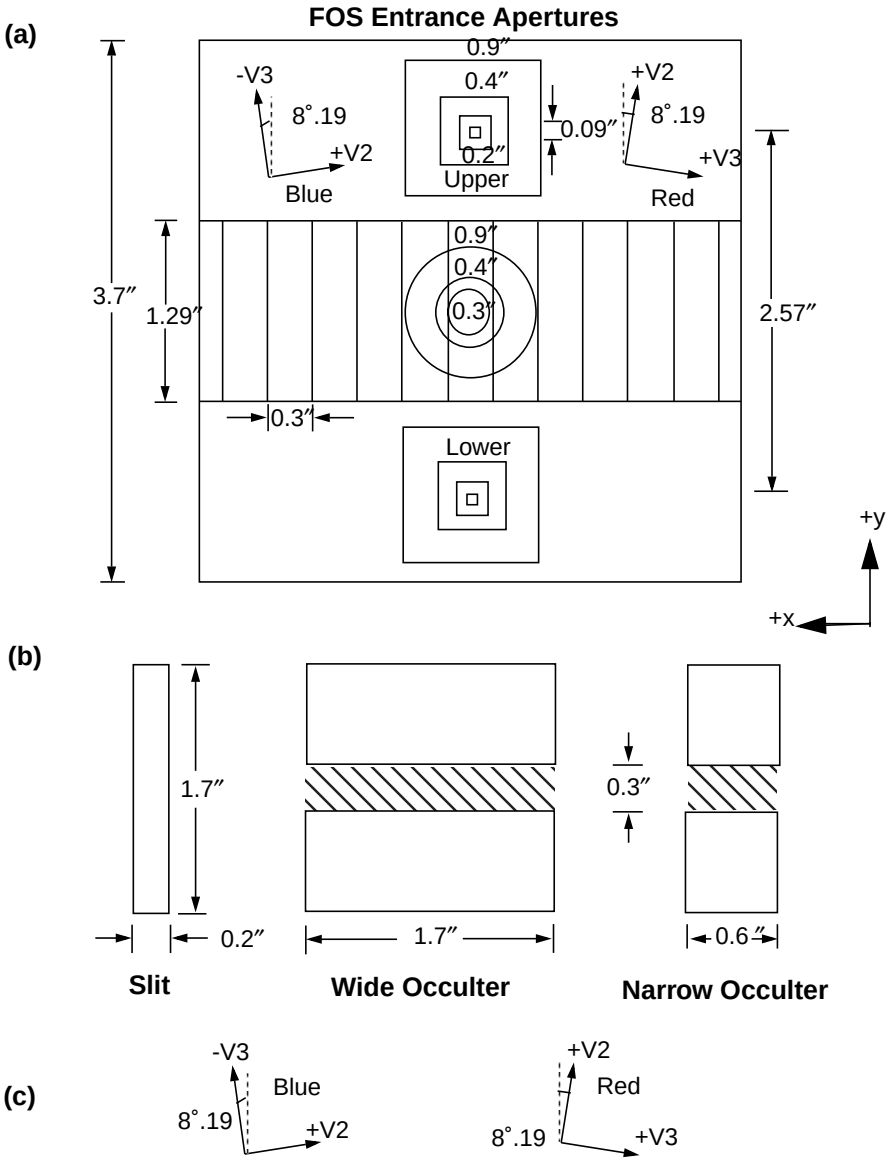

29.3.9 Data Acquisition Fundamentals

The FOS had several parameters that could be altered to change the way data was accumulated and read out. These parameters are summarized in Table 29.6.

To maximize the science data output from the FOS, routine data-taking commanding oversampled spectra and shifted the object spectrum with respect to the diode array during several subintegrations. These two procedures were called *substepping* and *overscanning*.

Table 29.6: Data Acquisition and Readout Parameters

Parameter	Description
INTS	Number of repetitions of the livetime/deadtime cycle, whereby electrons were counted in the selected diode accumulators with no changes in the magnetic deflection. Changing INTS provided a means for altering the amount of time data were collected at a given deflection value while keeing the livetime short so that as little good data as possible was rejected. The header keyword is INTS.
SUBSTEPS	Number of magnetic field deflections of the photoelectrons in the dispersion direction. The default value was 4 (quarter-stepping). The data went into new memory locations with each substep. The corresponding header keyword is NXSTEPS.
OVERSCAN	Number of times to repeat the addition of counts into the memory array. The accumulation in the memory array was such that data acquired from an offset of one diode was added at each overscan. Each offset was accompanied by a corresponding magnetic deflection in the dispersion direction so that the data from the photocathode location falls into the same memory location independent of the diode which sampled it. The default value of this parameter is 5. The purpose of overscanning was to average the response of the different diodes, including the dead diodes. The header keyword is OVERSCAN.
YSTEPS	Number of magnetic deflections of the electrons in the direction perpendicular to the dispersion. This parameter was used to map the photocathode (IMAGE mode), to switch between the two spectra produced by the polarizer, or to acquire either of the paired apertures. In the standard ACCUM mode this parameter had the default value of 1. The header keyword is YSTEPS.
SLICES/BIN	A slice consists of an entire deflection sequence. Data from each slice went to a new memory location. This was used for time resolved spectrophotometry. The header keyword is SLICE.
PATTERN	A pattern was a complete series of slices. Counts in subsequent patterns were added to the corresponding previous values in the data array. The header keyword NPAT determined the number of times a pattern should be executed to achieve the exposure time.
READOUT	A readout sent the science data to the CU/SDF computer for either storage on the tape recorder or for telemetry to the ground. FOS readouts were non-destructive and were performed at regular intervals (~4 min for the FOS/BL and ~2 min for the FOS/RD) without memory clears in order to protect against loss of data. The last readout contained all the data accumulated since the previous memory clear. In the standard ACCUM mode each readout is stored as a separate group in the data files.
Memory clears	A memory clear set to zero all locations in the science data array to allow input of new data. The number of times that a memory clear was repeated in a given observation is given in the NMCLEARS keyword.

Substepping was used to better sample the spectrum in the wavelength direction. This was necessary because a spectral resolution element mapped to a single diode, so critical sampling of the line spread function required substepping. *Overscanning* was used to assure that each pixel in the final spectrum contained data received from multiple diodes (to smooth out diode-to-diode variations and insure against data loss when a single diode was disabled). Both substepping and overscanning relied on the magnetic focus assembly in the Digicon detector to magnetically deflect the photoelectrons in the dispersion direction so that they fell on slightly different locations on the diode array.

For substepping, the spectrum was deflected by a fraction of a diode in the dispersion direction (where the fraction was given by 1/NXSTEPS and NXSTEPS is a header keyword; see Chapter 30). The diodes were read out into unique memory locations for each substep and the substepping was performed NXSTEPS times.

Figure 29.4: Approximate Location of Spectra on the Photocathode.
Dashed Lines Represent Red Detector, Solid Lines Represent Blue Detector

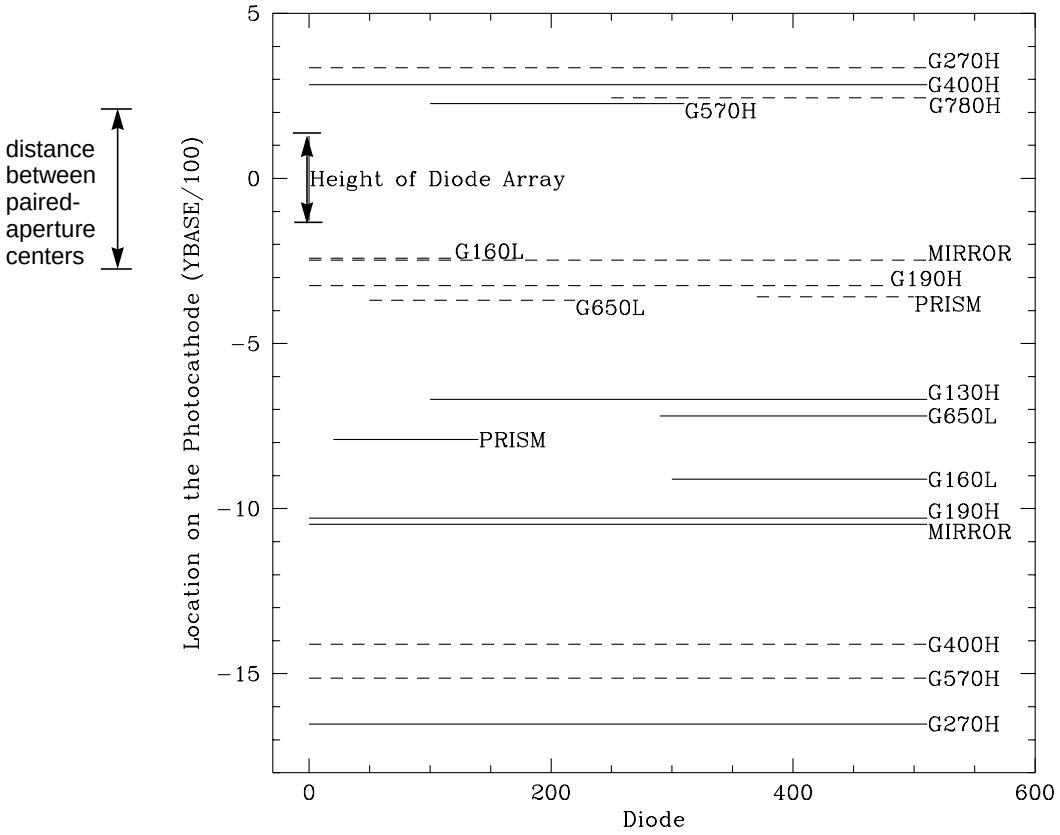

For *overscanning*, the process of substepping was continued over more than one diode in the dispersion direction. A complete round of substepping was performed for each overscan step. The number of overscan steps performed was determined by the overscan parameter (header keyword OVERSCAN). Each time a given wavelength position was deflected onto and measured by a new overscan diode, its counts were co-added into the same memory location in the FOS microprocessor. When using the full 512-element diode array, the result was a spectrum with 512 * NXSTEPS plus a small number (NXSTEPS x (OVERSCAN – 1)) of *edge* pixels. Each pixel (excluding the edge pixels) had data contributed from the number of diodes specified by OVERSCAN. Thus, substepping changed the number of pixels in the final spectrum; and overscanning principally changed the number of diodes that contributed to a single pixel. Although the number of diodes in the diode array was 512, the actual number of diodes read out could be restricted via a wavelength range specification in certain modes. The number of pixels in any observation is given by the equation:

$$\#\ of\ pixels = (\#\ of\ diodes + (\text{OVERSCAN} - 1)) \times \text{NXSTEPS}$$

Although other values could be specified, all FOS data acquisition modes, except ACQ/PEAK, used by default, NXSTEPS=4 and OVERSCAN=5. ACQ/PEAK observations used NXSTEPS=1 and OVERSCAN=1.

The default values of NXSTEPS=4 and OVERSCAN=5 yielded a typical spectrum of 2064 pixels in which a given diode contributed to the data in NXSTEPS x OVERSCAN, normally 20, consecutive pixels and a given pixel normally contained contributions from 5 adjacent diodes. The exposure time devoted to the first 2048 pixels (that is, all but edge pixels—described below) was 1/NXSTEPS (1/4) of the total exposure time specified for the observation.

Due to the nature of FOS overscanning, (OVERSCAN – 1) groups of NXSTEPS pixels at the +*x* edge of the diode array (long wavelength end for FOS/BL gratings and vice versa for FOS/RD) had contributions from fewer than OVERSCAN diodes. There were 16 such pixels in the default case, with the first four of these receiving 4/5 of the exposure of the first "normal" 2048 pixels, the next group of four receiving 3/5 of the typical exposure, the next four 2/5, and the last 4 1/5 of the normal pixel exposure. All standard pipeline routines within STSDAS and **calfos** handle these calculations automatically.

STScI FOS calibrations, which are described in chapter 31, support only OVERSCAN=5 observations. FOS calibrations are also designed for NXSTEPS=4, but may be easily adapted to all allowed values of NXSTEPS by a straightforward automatic resampling of standard NXSTEPS=4 reference files.

Note: Due to this FOS-specific substepping, the typical effective exposure *per pixel* in any FOS observation was the total observation exposure time divided by NXSTEPS. A few (i.e., NXSTEP*(OVERSCAN-1), typically 16, "edge" pixels had even less effective exposure.

29.3.10 Photon Counting Characteristics

The FOS Digicons were photon counting detectors. The output of the diodes was stored in 16-bit accumulators within the FOS microprocessor. These accumulators were readout at intervals defined by the detector and the data-taking mode, e.g., roughly every two minutes for FOS/RD ACCUM. Sufficiently bright sources could produce more than 65535 counts (2^{16}–1) in an interval and thereby suffer one, *or more*, occurrences of accumulator "wrap around." (see "unwrap" on page 33-11).

29.3.11 Other Characteristics

To minimize external influences on the magnetic deflection of electrons from the photocathode onto the diode array, both Digicons were magnetically shielded. However—especially for FOS/RD—the shielding was inadequate. Thus, telescope orientation relative to the Earth's magnetic field influenced the magnetic

deflection characteristics of the FOS. This produced a *geomagnetically induced image motion* (GIM, occasionally referred to as GIMP). A post-observation pipeline correction algorithm corrected for this effect *in the x-direction only* prior to April 5, 1993. In order to minimize this effect, on-board software was implemented on April 5, 1993, to compensate for this error in both detector coordinates. Residual uncertainties remained, however, which affected the calibration accuracy of the instrument, as described further in “Geomagnetically Induced Image Motion (GIM)” on page 32-14.

The FOS Y-bases—the amount of magnetic deflection necessary to direct the photoelectrons from the photocathode onto the diode array—did not remain constant over the FOS lifetime due to hysteresis in the repeated magnetization and de-magnetization cycling of the Digicons. The detectors accumulated residual magnetization over time that required progressively larger deflections to steer the photoelectrons onto the diode array. Uncertainties in the Y-base values remain an important limitation on photometric accuracy (see “Y-bases” on page 32-7 and “Image Centering (Image Location) Factors” on page 32-22).

29.3.12 Influence of COSTAR on FOS Data

COSTAR was installed in HST during the First Servicing Mission in December 1993 to correct the spherical aberration of the HST primary mirror. COSTAR restored the point spread function (PSF) to nearly the HST design specifications. Aperture throughputs were also dramatically improved. For example, the throughputs of the `4.3`, `1.0`, and `0.3` apertures increased by factors of 1.3, 2.0, and 2.5, respectively. The throughput increase for the `4.3` aperture was compensated to a large extent by losses due to the two additional reflections, but small aperture relative throughput improvements allowed much of the original FOS science program goals to be pursued post-COSTAR, particularly in those programs that required excellent small aperture PSFs and LSFs.

The two COSTAR correcting mirrors, M1 and M2, introduced a modest anamorphic magnification which differed by approximately two percent between COSTAR *x* and *y*. All aperture and pixel scales decreased to approximately 0.86 of their pre-COSTAR values. For example, the height of the diodes projected on the sky changed from 1.43" pre-COSTAR to 1.29" post-COSTAR.

Between December 28, 1993, and February 1, 1994, numerous adjustments were made to the COSTAR mirrors. No effective instrumental calibration is available for any FOS data taken in that time period. By February 1, 1994, the COSTAR FOS-correction mirrors had been optimally aligned. The post-COSTAR FOS instrumental configuration that is calibrated by STScI began on February 1, 1994.

Throughout most spectral regions COSTAR introduced only moderate modifications to the wavelength dependence of instrumental sensitivity, however, an unanticipated broad decrease in instrumental sensitivity was recorded for FOS/BL in the wavelength range 1600–2400 Å. This feature was roughly Gaussian in shape and at 2000 Å. the post-COSTAR sensitivity was approximately 70% of its expected post-COSTAR value.

Additionally, the narrower post-COSTAR PSF more selectively illuminated fine-scale photocathode granularity rather than smoothing it out as was the case with the aberrated PSF. As a result, very precise target acquisitions became an important requirement for both science and calibration programs that needed to achieve high flatfielding accuracy.

The narrower PSF also led to a narrower line spread function (LSF) for post-COSTAR data compared to the pre-COSTAR era. Polarimetric data were affected, because additional optical elements (mirrors) were introduced into the light path, and this changed the characteristics of the incoming wavefronts. On the other hand, the internal wavelength calibration was not measurably affected, although some indication of grating-dependent internal-to-external wavelength offset changes was seen.

29.4 Science Observing Modes

The FOS employed one of six basic data taking modes to acquire science data:

- Spectrophotometry (ACCUM).
- Rapid Readout (RAPID).
- Time-Resolved Photometry (PERIOD).
- Spectropolarimetry.
- Image.
- Paired Aperture Observing.

ACCUM was by far the most commonly used observing mode. In this section we provide basic descriptions of each of these science data taking modes and their scientific uses. More detailed discussions of each instrument mode including operational characteristics, the diagnostic paper products, the structure of the electronic data products and methods of data quality analysis are provided in Chapter 30.

29.4.1 Spectrophotometry Mode (ACCUM)

ACCUM was the standard FOS spectrophotometric data taking mode. Data were acquired with NXSTEPS=4 and OVERSCAN=5 only. Spectra were read out at approximate 2 minute (FOS/RD) or 4 minute (FOS/BL) intervals and the accumulated sum after each read was stored and recorded in consecutive groups in the standard output data files (see next chapter for description of these files). Therefore, each consecutive spectrum was made up of the sum of all previous intervals of data in an ACCUM observation.

29.4.2 Rapid Readout Mode (RAPID)

Observations requiring higher time resolution than that provided by ACCUM mode used RAPID mode in which the diode array was read out at a rate set by the observer. Readout rates as fast as 0.033 sec were possible (0.035 sec was the fastest ever implemented). NXSTEPS=1, 2, or 4 and OVERSCAN=5 (or, rarely, 1) were normally used, though the full set of commandable values was available. The actual percentage of specified dwell time that was spent exposing could vary substantially depending upon how instrumental parameters were chosen. Timing precision more accurate than 0.125 seconds requires special analysis of engineering data stream information (see timing discussion in Chapter 33). Unlike ACCUM, the actual spectrum obtained in each individual time interval was recorded in the output data products.

29.4.3 Time-Resolved Spectrophotometry (PERIOD)

As a result of implementation errors there were no fully successful PERIOD mode observations made in the FOS science program. Successful tests were performed during Science Verification.

This mode was designed for objects with known periodicity in the 50 msec to 100 sec range. To maintain the phase information of these observations, the known period (CYCLE-TIME) of the object was divided into *bins* or *slices*, where each bin had a duration time = period / bins. The spectra acquired in this mode were stored in the different bins which corresponded to a given phase of the period. The spectral information obtained in each period cycle was added to the appropriate phase bin (so long as the period was known accurately). Onboard memory limitations placed substantial restrictions on the number of diodes that could be read out and the number of phase bins that could be sampled.

29.4.4 Spectropolarimetry Mode

Polarimetry data consist of a number of consecutive ACCUM-like exposures (POLSCAN=16, 8, or 4) with the waveplate set at POLSCAN different angles (all within one target visibility period). The Wollaston prism split the light beam into two spectra corresponding to the orthogonal directions of polarization. Although SINGLE apertures were always used, both spectra illuminated different portions of the photocathode—one above, one below the standard SINGLE aperture Y-base location for the disperser employed. Hence, each exposure consisted of the two orthogonal spectra obtained with a single waveplate angle. The first spectrum corresponded to the first pass direction (ordinary ray), the second to the second pass direction (extraordinary ray). These spectra were deflected alternately (*not simultaneously*) onto the diode array, recorded as the two pass directions, and stored as a single group in the raw data file. The total exposure time specified in the exposure logsheet was divided equally among each of the POLSCAN steps with one-half of the resultant exposure times spent observing each pass direction. These requirements, combined with large instrument overheads, placed tight limits on the length of any individual polarizer position exposure.

Chapter 32 discusses how Y-base positional uncertainties and GIM effects, coupled with the large pre-COSTAR PSF and the influence of the additional reflections in COSTAR, limited the accuracies of FOS polarimetric observations.

29.4.5 Image Mode

IMAGE mode observations could be made with either the camera MIRROR (as in ACQ images discussed above) or with a disperser in the beam. Normally IMAGE mode observations used NXSTEPS=4 and OVERSCAN=5, but the full set of commandable values were available. In IMAGE mode observations both the number and length of rasters and the *y*-position of each raster could be specified, so that: 1) a white-light image of all or a portion of the aperture was possible with the MIRROR, and 2) spectra from different portions of the aperture were sampled with a disperser.

ACQ mode images, discussed above, simply used a pre-defined, optimized set of IMAGE mode parameters. Most dispersed light IMAGE mode observations were made for specialized calibration purposes, but this mode was occasionally used for interactive target acquisitions of moving targets (the so-called dispersed light interactive target acquisition technique).

29.4.6 Science Data-Taking with Paired Apertures

Depending upon the value of the STEP-PATT RPS2 (RPSS) parameter, paired aperture observations could invoke a different detector readout pattern from that employed for single apertures for ACCUM and RAPID exposures. In certain circumstances (see next chapter) readout deflections were alternated equally between upper and lower paired apertures at approximate 10 second intervals for the duration of the exposure. An additional, but never used, pattern allowed such upper and lower aperture samplings and an additional background sample halfway between the apertures.

29.5 Target Acquisition

In order for FOS to have observed a target, that target must, naturally, have been located in the instrument aperture. Several techniques for positioning the target in the aperture were available to FOS observers, including:

- ***An FOS Onboard target acquisition:*** Used either a Binary Acquisition (ACQ/BINARY), a Peakup or Peakdown (ACQ/PEAK), an interactive acquisition (INT ACQ), an early FOS Image (ACQ) or a firmware acquisitions (ACQ/FIRMWARE).

- ***Blind pointing*** (i.e., observe at the telescope pointing immediately following the guide star acquisition without further refinement of telescope position). This was rarely used because the one sigma accuracy was on the order of 1".
- ***GHRS-assisted acquisition***: GHRS could be used to acquire an object followed by slew and additional centering with FOS. This option was rarely used as the equivalent FOS overheads were more efficient. Conversely, FOS-assisted acquisitions for GHRS were common in Cycles 5 and 6 (see *GHRS ISR* 068 and *FOS Instrument Handbook* version 6 for details).
- ***WF/PC1-assisted acquisition***: Similar in principle to GHRS-assisted acquisition except centering slew calculated on ground after WF/PC-1 exposure. Rarely used, this option was only available pre-COSTAR (prior to December 15, 1993).
- ***Reuse target offset***: In order to avoid unnecessary overhead times, a new technique was developed for proposals that required more than one visit to a target within a few days (up to two months). This *reuse target offset* method, first employed in December 1994, allowed the instrument to use a target offset that was derived in the acquisition for an initial visit during subsequent visits so that these later visits need use only a single-stage peak-up/peak-down acquisition to reconfirm the correct centering of the target in the aperture. Limiting accuracies of 0.03" were commonly achieved.

The overwhelming majority of FOS target acquisitions used the onboard acquisition modes ACQ/BINARY and ACQ/PEAK. A brief description of each of the FOS acquisition modes is provided below, and a more complete description of the acquisition modes, the data they produced and how to determine the target centering accuracy for a particular observation is provided in “Assessing FOS Acquisitions” on page 30-26.

Researchers will want to remember that FOS instrument performance (flatfields and sensitivity, especially) is best understood for the very center of the apertures. The accuracy inherent to the target acquisition strategy employed will therefore determine the calibration accuracy that can later be reached with a particular dataset. For each set of FOS observations of a given source, the first dataset taken was the FOS target acquisition image.[2]

The target acquisition employed for a given observation will determine the accuracy of the target centering in the science aperture, which in turn affects the calibration accuracy of the science data itself. Analysis of FOS observation data quality is incomplete without retrieval and assessment of the target acquisition exposures.

2. If a blind pointing was done, there will not have been a target acquisition image, unless one was specifically requested.

29.5.1 FOS Onboard Acquisitions

BINARY acquisition (ACQ/BINARY)

In a BINARY acquisition, single raster images of the target were made with the MIRROR in each of the upper, middle, and lower thirds of the 4.3 aperture. The aperture segment containing the brightest image was determined and the brightest pixel provided the *x*-position of the target. Next a scheme involving a series of up to eight successively smaller electronic deflections was employed to find the Y-base that placed the target on the edge of the diode array. During this procedure all image offsets were performed electronically—the target was not moved until the actual aperture centering slew was calculated by the algorithm. Due to its efficiency (but with limited centering accuracy), ACQ/BINARY was the acquisition method of choice for point sources fainter than V~15 in programs for which S/N < 30 was sufficient. The method had a restricted dynamic range of brightness and, in the pre-COSTAR period, was severely limited by the aberrated PSF. Acquisition of faint sources that required high pointing accuracy often began with ACQ/BINARY and concluded with one or more ACQ/PEAK sequences.

Peakup or Peakdown Acquisition (ACQ/PEAK)

In an ACQ/PEAK sequence, NXSTEP=1 integrations were performed at a series of defined positions on the sky with a science aperture and either MIRROR or a disperser in place. At the end of the slew sequence, the telescope was returned to the position with either the most (peakup) or fewest (peakdown) counts (return to brightest or return to faintest). Overheads for ACQ/PEAK slew patterns were large (30-45 seconds per dwell). ACQ/PEAK was generally required for the following types of observations:

- All exposures requiring S/N>30.
- High wavelength accuracy.
- Pointing more accurate than 0.2".
- Objects too bright to acquire with the MIRROR.
- Objects too variable to acquire with ACQ/BINARY.
- Centering targets in apertures smaller than `1.0`.
- Positioning bright sources behind the occulting bars.

Interactive Acquisition Image (INT ACQ)

In an interactive acquisition, the camera MIRROR was used to obtain an image of the `4.3` aperture field. The image was downlinked and analyzed in real time to determine the required slew to center the target. The slew was uplinked and FOS science observations proceeded, generally at the start of the next target visibility. This method was employed for a number of moving target acquisitions.

Early FOS Acquisition Image (ACQ)

When taking an early FOS acquisition image, a camera MIRROR image of the `4.3` aperture was acquired in similar fashion to that described for INT ACQ above, but, in this case, the science observations were performed at a later date. Often the early FOS image was used to determine geometry of crowded fields or

precise offsets from a nearby bright target likely to be acquired by ACQ/PEAK or ACQ/BINARY.

Firmware Acquisition (ACQ/FIRMWARE)

Firmware acquisition was an engineering mode that mapped the camera MIRROR image of the `4.3` aperture in *x* and *y* with small, selectable *y* raster increments. The microprocessor filtered this aperture map in real time and found *y*-positions of the peaks by fitting triangles through the data. ACQ/FIRMWARE was less efficient than ACQ/BINARY and failed if more than one object were found. This mode was used for a small number of pre-COSTAR planetary satellite acquisitions and was not used in the post-COSTAR science program.